AN INTEGRATED CHIP COIL SENSOR AND INSTRUMENTATION AMPLIFIER FOR BIO-MAGNETIC SIGNAL ACQUISITION

Vijith Vijayakumaran Nair, Jin Hwan Youn and Jun Rim Choi
School of Electronics Engineering, Kyungpook National University,
Daegu, South Korea, 702-701.

ABSTRACT

This paper presents a miniaturized magnetic sensor chip for bio-magnetic signal measurements. The sensor fabricated in 0.18 μm CMOS process embeds an inductance coil and instrumentation amplifier that provides excellent sensitivity and low reference noise level in comparison to the state of art. The integrated sensor with frequency band between 50 Hz and 5 KHz illustrates bandpass filter characteristics which attenuates the low and high frequency noise from the external environment. The signal sensitivity of the device is 3.2 fT/μV and inferred noise at 300 Hz is 29 fT/$\sqrt{}$Hz. The sensor is used for bio-magnetic signal acquisition.

KEYWORDS

Integrated Chip, Sensor Coil, Instumentation Amplifier, Biomagnetic signals.

INTRODUCTION

In practical measurements of bio-magnetic signals, there are many difficulties associated to mensuration performance especially when the magnetic field is weak. In general SQUID sensors are employed to measure bio-magnetic signals with multichannel based systems [1], [2]. However, the magnetic field generated by source body is weak and negligible in comparison to the surrounding devices at the time of measurement. Hence, separation of the bio-magnetic signal from external noise is a difficult task. Also, crosstalk between the multichannel device also affects the signal acquisition [2]. Moreover sensors like the magnetoresistive sensors are bulky and less sensitive (120 fT/$\sqrt{}$Hz at 1 KHz) [3], optical pumped magnetometers are both complex and expensive [4] and also the fluxgate magnetometers with low sensitivity (500 fT/$\sqrt{}$Hz at 1 KHz) [4], are less suitable for the purpose of detecting bio-magnetic fields. To overcome the performance and design issues of prior works [1], [2], [3], [4], and to aid portability of the device, a high inductance coil sensor that couples a large quantity of flux is designed for detecting weak magnetic fields specifically bio-magnetic fields. An induction coil sensor [4], [5], [6], [7], [8], detects the voltage induced by the magnetic flux linkage in a coil. The developed voltage is picked up by the instrumentation amplifier (IA) and processed further. In consideration to the high input resistance of the IA, majority of the AC voltage generated by the coil is transferred to the IA. This paper presents the design and development of high inductance coil sensor and an IA based on integrated chip platform for bio-magnetic signal measurements.

HIGH INDUCTANCE COIL SENSOR

In general coil sensor has greater sensitivity over hall sensor and magnetic resistance sensor when integrated on to chip [1], [2], [4], [5]. Coil sensors can measure up to 1 pT [4], [6], [7], [8]. The induction coil sensor works on the fundamentals of Faraday's law. It states that a change of magnetic flux density through the coil induces a voltage across coil and is proportional to rate of change of density. The transfer function is given as:

$$V = -n \cdot \frac{d\phi}{dt} = -n \cdot A \cdot \frac{dB}{dt} = -\mu \cdot n \cdot A \cdot \frac{dH}{dt} \qquad (1)$$

where ϕ is the magnetic flux through the coil, n the number of turns and A the coil active area. The voltage developed across the coil is picked up by the IA as the input resistance of IA is comparably high to that of the high inductance coil sensor. The coil sensor is designed based on optimization in magnetic field simulation tool. Feature size optimization of the coil is based on the trade-off between the cutoff frequency and noise characteristics. With constant external diameter, an increase in internal diameter decreases the cutoff frequency, but decreases the sensitivity and increases the noise. The increase in the noise is due to the interaction of earth's magnetic field with the coil. As the internal diameter is increased, the earth's magnetic field passing through the coil increases, thus increasing the noise [5]. On contrary, for specific external diameter, if internal diameter is decreased, cutoff frequency increases, sensitivity increases and the noise figure decreases.

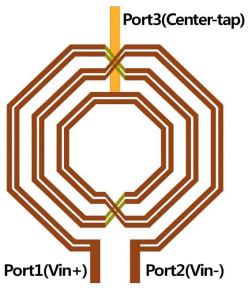

Figure 1: Schematic model of the designed coil for 3 turns.

The high inductance coil designed is a differential planar multi-path octagonal shaped spiral coil as in figure 1. It is designed by employing two adjacent metal layers on the silicon substrate. The design based on multi-path technique increases Q-factor and inductance of the coil in comparison to single path coil [9]. Stacked single path coils can be also fabricated in 0.18 μ CMOS process with 5 metal layers. But, for differential multi-path coils it is not a recommended option due to the capacitive interactions between the adjacent layers. Besides, the stacked coil modelling and simulation process in electromagnetic tool is more complex and results are inconsistent [10]. The modelled multi-path coil for three turns is shown in the Figure 1. Simulation results of the coil depicts typical high-pass filter (HPF) characteristics. At low frequency Q-factor decreases rapidly but for moderate

and high frequency after the cutoff frequency the increase is small and gradual. The cutoff frequency is determined in prior to the fabrication of the coil by simulation process, so as to optimize the coil sensor for maximum sensitivity and minimum cutoff frequency. The Q-factor of the simulated coil is shown in Figure 2.

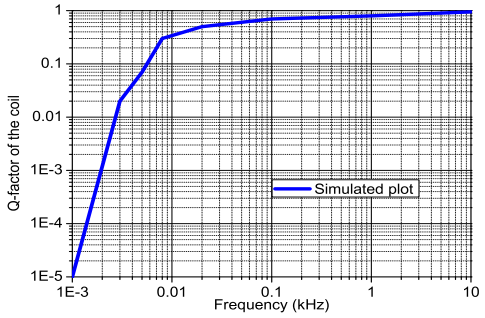

Figure 2: Q-factor variation of the coil with frequency.

INSTRUMENTATION AMPLIFIER

In bio-magnetic signal acquisition, separation of original signal from the background noise is a difficult task. Thus, noise reduction is the integral part of the design approach. A band pass filter (BPF) approach is advisable for the design [11], [12]. The design helps to suppress the low frequency noise from the human body and the high frequency noise from the surrounding. The proposed IA is based on current feedback technique [11], [12], [13], [14] and comprises of a low G_m operational transconductance amplifier (OTA) to achieve high CMRR with HPF characteristics. IA consists of an initial transconductance stage, a transimpedance stage, a g_m tuned OTA based high pass filter, a common mode feedback (CMFB) circuit and biasing circuit for the IA. The block diagram of the IA is shown in figure 3.

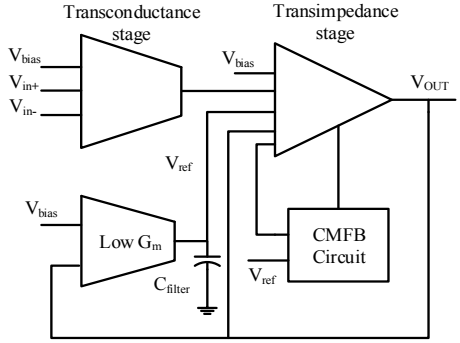

Figure 3: Block diagram of the instrumentation amplifier.

Input differential voltage V_{in+} and V_{in-} are converted into a differential current, I_1, flowing through R_1. The current mirror circuit, mirrors I_1 to I_2, and the output voltage is given by I_2*R_2. But, when the DC offset voltage becomes a non negotiable factor the final output voltage is given by:

$$V_{out} = \frac{R_2}{R_1}(V_{in+} - V_{in-}) + V_{Ref} + V_{offset} \qquad (2)$$

The IA includes, CMFB circuit to compensate generated DC offset voltage at the output. The circuit schematic of

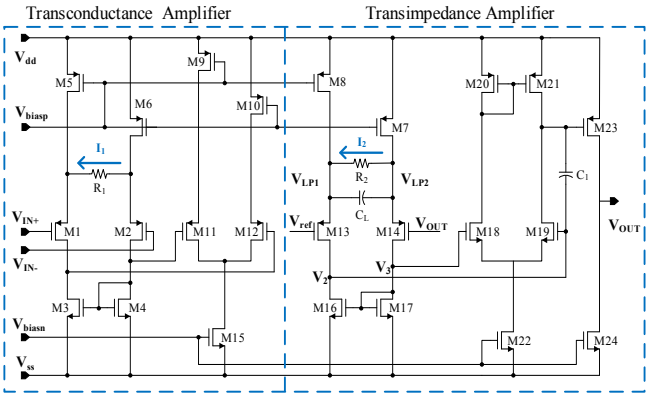

Figure 4: Schematic dig. of the instrumentation amplifier.

the proposed OTA is shown in figure 4. To reduce flicker noise, p-type transistors are used as input transistors [9]. For bio-magnetic signal acquisition, the CMRR of the IA is designated to be larger than 90 dB and input referred noise lower than 10 μV RMS [9]. Acquisition of signals in the frequency range between 0.5−5000 Hz corresponds to bio-magnetic signal band. For the low pass filter (LPF) formed by the R_2 and C_L in the main amplifier stage, the corresponding 3 dB cutoff frequency is given by:

$$f_H = \frac{1}{2\pi R_2 C_H} \qquad (3)$$

The HPF filter aids the attenuation of low frequency noise from the human body. An approach based on G_m−C that can achieve sufficiently large impedance replaces HPF, as it reduces area cost in absence of resistance [11], [12], [13], [14]. Though the G_m−C filter achieves low −3 dB cutt-off frequency at 0.5 Hz as in equation 4, for the feedback from V_{out} to HPF, C_H is too large to integrate on the die.

$$f_L = \frac{G_m}{2\pi C_L} \qquad (4)$$

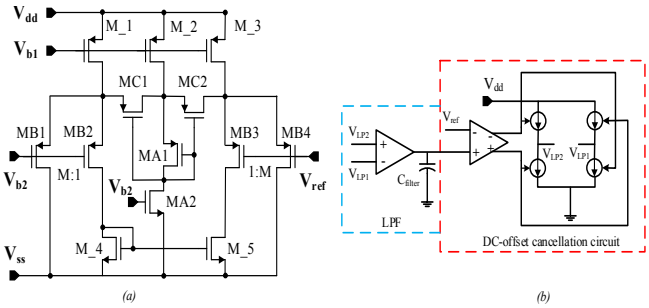

Figure 5: Schematic of the (a) OTA (b) CMFB circuit.

From equation 4, to reduce filter capacitor size, lowering the G_m is an advisable technique. A small G_m OTA based on current division technique as shown in figure 5(a) is utilized to tune the G_m. The small signal transconductance of the OTA is expressed as in equation 5.

$$G_m = \frac{g_0 MC}{M+1} = \frac{1}{M+1}(\mu_n C_{ox}\frac{W}{L}(V_G - V_{CM} - V_T)) \qquad (5)$$

Where, g_0MC is the conductance of MC1 and MC2, M is the width ratio of MP1 to M1P, μ_n the mobility of the carrier, C_{ox} is gate-channel capacitance, V_G the gate voltage, V_{CM} the common mode voltage, V_T the threshold voltage. In order to compensate for the increase in output DC offset voltage, a CMFB circuit is implemented along with the LPF as shown in figure 5(b). The bias circuits are designed as in [15]. The IA in total act as an BPF with -3 dB bandwidth from 0.5-5000 Hz.

IMPLEMENTATION RESULTS

The designed high inductance coil sensor and IA is fabricated in 0.18 μm TSMC process. Figure 6 shows the simulated and measured inductance value of the fabricated coil with respect to varying frequency. As the resonant frequency of the planar coil is in the range of MHz, the inductance variation is very small at lower frequency, which is our operational frequency band. The multi-path spiral inductor provides a higher magnitude of inductance in comparison single path spiral coil designed. The summary of the measured coil parameter is depicted in the table 1.

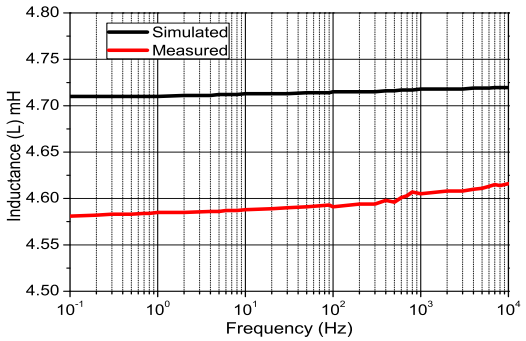

Figure 6: Measured and simulated inductance curve.

Table 1: Measured sensor coil parameters.

Characteristics	Value
Technology	0.18 μm CMOS process
Q- factor of coil	0.28 at 100 Hz
Resistance of the coil	42.4 KΩ
Capacitance of the coil	138 pF at 100 Hz
Area occupied by the coil	3.6 mm x 3.6 mm
Number of turns	901

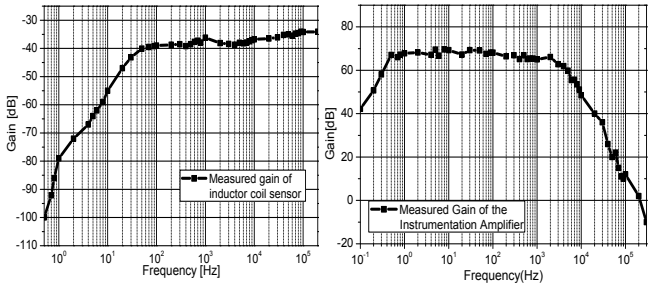

(a) *(b)*

Figure 7: Measured gain of (a) coil (b) IA.

The total system works by summing the gain of the coil sensor and the IA. Thus, sensor coil gain is an integral part of the measurement procedure. The gain measurement of the coil sensor to change in frequency is given in figure 7(a). The figure 7(a) indicates the frequency characteristics of a HPF. It shows that gain increases by approximately 25 dB/dec when traversing from low to high frequency and at a particular frequency (50 Hz) the shows a flat curve proceeding towards higher frequencies.

The IA in the fabricated chip operates as a BPF, with a frequency bandwidth in between 0.5−5000 Hz. Frequency response of the IA is shown in figure 7(b). The measurement data indicates a maximum mid-band gain of 70 dB and maximum CMRR of 128 dB is achieved. To integrate the filter capacitor on the chip, the G_m of the low G_m OTA is tuned appropriately. Table 2 shows the performance comparison of the fabricated IA to prior artworks.

Table 2: Performance comparison of prior IAs.

	[10]	[10]	[10]	This work
Technology	0.18 μm	0.35 μm	0.8 μm	0.18 μm
Supply Voltage	1 V	3 V	3.3 V	3.3 V
CMRR	124 dB	110 dB	80 dB	128 dB
Gain	46 dB	50 dB	50.5 dB	68 dB
Power	165 μW	4.9 μW	n/a	84 μW
Input referred noise (RMS)	2.8 μV	n/a	0.95 μV	0.87 μV

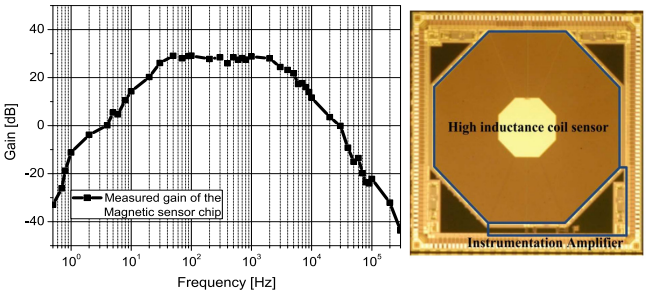

(a) *(b)*

Figure 8: (a) Measured gain (b) Die-micrograph of sensor.

Together with the gain of the sensor coil and the IA a BPF is formed with lower -3 dB cutoff frequency of 50 Hz and upper -3 dB cutoff frequency 5000 Hz. Figure 8(a) shows the combined gain of the high inductance coil sensor for varying frequency. The maximum mid-band gain of the chip is 30 dB at 100 Hz. For noise analysis an input signal of 1 kHz generated in the coil is applied to IA that resulted in output signal of 515 mV_{rms}, noise voltage of 6.48 μV_{rms} and 97 dB signal-to-noise ratio (SNR). The measurement details are depicted in figure 9(a). The performance analysis of sensor is done creating magnetic field in reference coil and using EHP-50C electric and magnetic field analyzer as reference, the sensor is calibrated. The measurement results indicate sensitivity of 3.25 fT/μV. The noise analysis shows 29 fT/$\sqrt{\text{Hz}}$ inferred at 300 Hz. Table 3 shows a property comparison of the existing artworks to the proposed work.

For verification by experiment, bio-magnetic signals are measured for process of muscle contraction and relaxation for a period of 10 s. The measurement results indicate 52

mV_{rms} during muscle contraction and 32 mV_{rms} for muscle relaxation. The experimental result is depicted in figure 9(b).

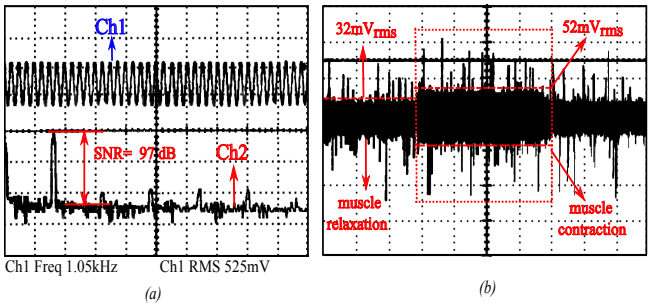

Figure 9: Experimental (a) Noise analysis (b) Test results.

Table 3: Performance comparison of prior Sensors.

	SQUID sensor Elekta Neuromag	**[1]**	**This work**
Bandwidth	10 Hz to 5 KHz	30 mHz to 300 KHz	50 Hz to 5KHz
Sensitivity	1-10 fT/μV	n/a	3.25 fT/μV
Noise	3 fT/$\sqrt{}$Hz at 6 Hz	40 fT/$\sqrt{}$Hz at 300 Hz	29 fT/$\sqrt{}$Hz at 300 Hz
Gradiometer	26.8x10 x17 mm^3	18x300 mm^2 235g	5 x 5 x 0.2 mm^3
Coil Area	21x21 mm^2	10x9 mm^2	3.2x3.2 mm^2

CONCLUSION

The paper presents the design and fabrication of a high inductance coil sensor and IA for bio-magnetic signal acquisition. The proposed multi-path planar inductor and IA is fabricated in 0.18 μm CMOS technology. The inductor coil sensor replicates HPF response and the IA with low G_m shows BPF characteristics. Together with the coil sensor and the IA forms a BPF with lower and higher -3 dB cutoff frequency of 50 Hz and 5 KHz respectively. The fabricated sensor recovers the bio-magnetic signals with this band. The implemented IA exhibits high CMRR of 128 dB with low input referred noise of 0.87 μV_{rms}. The sensor system in comparison to prior works, occupies relatively smaller area and thereby increases the portability of system for bio-magnetic signal acquisition. Future works include the system design for acquisition of signals for very low frequency range and improving the signal integrity. The fabricated device can be applied for medical systems.

ACKNOWLEDGMENT

This work was supported by the Korea Science and Engineering Foundation (KOSEF) grant funded by the Korean Government (MOST) (No.2013R1A1A4A01012624) and Kyungpook National University Research Fund 2013(2014).

REFERENCES

[1] R. J. Prance, T. D. Clark and H. Prance "Compact room-temperature induction magnetometer with superconducting quantum interference device level field sensitivity," *REVIEW OF SCIENTIFIC INSTRUMENTS*, vol.74, no.8, pp. 3735–3739, 2003.

[2] S. Rombetto, C. Granata, A. Vettoliere and M. Russo "Multichannel System Based on a High Sensitivity Superconductive Sensor for Magnetoencephalography," *Sensors*, vol.14, pp. 12114–12126, 2014.

[3] S. X. Wang and G. Li "Advances in Giant Magnetoresistance Biosensors With Magnetic Nanoparticle Tags: Review and Outlook," *IEEE TRANSACTIONS ON MAGNETICS*, vol.44, no.7, pp. 1687–1700, 2008.

[4] S. X. Wang and G. Li "Induction coil sensorsa review," *MEASUREMENT SCIENCE AND TECHNOLOGY*, vol.18, pp. 31–46, 2007.

[5] J. Malmivuo and R. Plonsey, *Bioelectromagnetism - Principles and Applications of Bioelectric and Biomagnetic Fields*, Oxford University Press, 1995.

[6] A. Grosz and E. Paperno, "Analytical Optimization of Low-Frequency Search Coil Magnetometers," *IEEE SENSORS JOURNAL*, vol.12, no.8, pp. 2719–2723, 2012.

[7] K. Tashiro, "Optimal Design of an Air-core Induction Magnetometer for Detecting Low-Frequency Fields of Less than 1 pT," *IEEE SENSORS JOURNAL*, vol.30, pp. 439–442, 2006.

[8] B. Yan, W. Zhu, L. Liu, K. Liu and G. Fang, "An Optimization Method for Induction Magnetometer of 0.1 mHz to 1 kHz," *IEEE TRANSACTIONS ON MAGNETICS*, vol.49, no.10, pp. 5294–5300, 2013.

[9] X. Xu, P. Li, M. Cai and B. Han, "Design of Novel High-Q-Factor Multipath Stacked On-Chip Spiral Inductors," *IEEE TRANSACTIONS ON ELECTRON DEVICES*, vol.59, no.8, pp. 2011–2018, 2012.

[10] J. Zhao, "A new calculation for designing multilayer planar spiral inductors," Pulse, EDN Network, 2010.

[11] R. Martins, S. Selberherr and F. A. Vaz, "A CMOS IC for Portable EEG Acquisition Systems," *IEEE TRANSACTIONS ON INSTRUMENTATION AND MEASUREMENT*, vol.47, no.5, pp. 1191–1196, 1998.

[12] H. Wu and Y. P. Xu, "A Low-Voltage Low-Noise CMOS Instrumentation Amplifier for Portable Medical Monitoring Systems", *IEEE-NEWCAS Conference*, pp. 295-298, 2005.

[13] C. Nanda, J. Mukhopadhyay, D. Mandal, and S. Chakrabarti, "A CMOS instrumentation amplifier with low voltage and low noise for portable ECG monitoring systems," *IEEE Int. Conf. on Semiconductor Electronics*, pp. 54-58, 2008.

[14] C. Nanda, J. Mukhopadhyay, D. Mandal, and S. Chakrabarti, "Analysis of Op-Amp Power-Supply Current Sensing Current-Mode Instrumentation Amplifier for Biosignal Acquisition System ," *30th Annual International IEEE EMBS Conference*, pp. 2295-2298, 2008.

[15] D. Johns and K. Martin, *Analog Integrated Circuit Design*, John Wiely and Sons, 1997.